Bright and exotic solitons in laser cavity with frequency selective feedback

BALDEEP KAUR[a], SOUMENDU JANA[a,*], QIN ZHOU[b], ANJAN BISWAS[c,d], MILIVOJ BELIC[e]
[a]*School of Physics and Materials Science, Thapar University, Patiala, Punjab-147004, India.*
[b]*School of Electronics and Information Engineering, Wuhan Donghu University, Wuhan, 430212, P.R. China*
[c]*Department of Mathematical Sciences, Delaware State University, Dover, DE 19901-2277, USA*
[d]*Department of Mathematics, Faculty of Science, King Abdulaziz University, Jeddah-21589, Saudi Arabia*
[e]*Science Program, Texas A & M University at Qatar, PO Box 23874, Doha, Qatar*

Soliton solutions are obtained in a vertical cavity surface emitting laser coupled with frequency selective feedback. Bright and exotic solitons (with cosh-Gaussian pulses) solutions are derived. The complex Ginzburg-Landau equation, with cubic nonlinearity, governs the soliton dynamics in the cavity. He's semi-inverse Variational method is implemented to retrieve these soliton solutions. A parametric region, which corresponds to stable soliton propagation, has been identified. The cosh-Gaussian soliton solutions can be a used to realize all-optical tunable devices and study cavity soliton in the system.

1. Introduction

Spatial dissipative solitons (SDS) are self-localised structures on a spatially extended system that is far from equilibrium [1-4]. Dissipative solitons (DS) appear as a discrete family of bound states. These are observed in numerous systems such as in nonlinear optics [1-4], fluid dynamics [5], ferrofluids [6], gas discharge [7], granular media [8], different lossy biological [9] and chemical systems [10] and even in nature [11]. A nice review on DS can be found in reference [12] and the references therein, while the reference [13] elucidates the diversity of such soliton. DS are significantly different but more general in comparison to that arises in a conservative system. For instance, in a conservative optical system spatial soliton is obtained when self-diffraction of the laser beam is balanced by means of nonlinearity induced self-focusing [14]. In a dissipative system, in addition to the aforesaid balance, it is required to compensate the inevitable loss of the system with some gain to achieve a soliton [15]. Since this kind of soliton is obtained in a dissipative environment they are generally referred as dissipative solitons, although other names like dissiton [16], 'auto soliton' [17] have been coined. Due to the requirement of the additional balance DSs are obtained in discrete parametric zone. The main requirement for the survival of DS is the constant supply of energy from the external source. Optical DS has been widely investigated in laser cavity, particularly in vertical cavity surface emitting laser (VCSEL). Experimental demonstration of optical DS are though rare until recent past [18-20], theoretical investigation witnessed huge advancement in the field [21- 23]. In order to keep the solitons 'alive' inside the laser cavity, a gain mechanism

is required. This gain mechanism can be provided by several means, namely, optical injection in the form of holding beam, frequency selective feedback using Bragg's grating [20] or using a saturable absorber [21]. In the present model we compensate the loss in VCSEL by using frequency selective feedback (FSF) [22, 23]. For mathematical modelling of such dissipative systems complex Ginzburg-Landau equations (CGLE) are widely used [22, 24, 25]. Some work used perturbed nonlinear Schrödinger equation (NLSE) as a model [26]. It is worthy to mention that the CGLE can be considered as a perturbed NLSE [27]. Here, we consider a CGLE which describes a realistic model of the VCSEL in conjugation with FSF. This may yield a special kind of optical dissipative soliton, called cavity soliton. However, we confine our investigation to traveling wave solution only. Cavity soliton can be viewed as a soliton confined between the cavity walls. Ref. [28] provides the evidence that a VCSEL with FSF supports cavity solitons, which aroused as localized traveling waves on homogenous stable non-lasing background. Necessarily, a TW needs to fulfil few standard criteria to be referred as a CS. Namely, it should show exponential localization at any point of the spatially extended system and exhibit bistability, i.e., being 'on' or 'off' in the same condition. Here, we find the traveling wave soliton solution of the system in the presence of dissipation using He's semi-inverse variational method [29-32]. It's an appreciated method to find traveling wave solution in a wide variety of systems including nanofibers [33]. Besides Kerr nonlinear media, the suitability of this method now is established in studying optical soliton perturbation in media having different nonlinearities, namely, non-Kerr-law nonlinearity [34], dual power-law nonlinearity [35] and log-law nonlinearity [36]. In addition to provide the best suitable solution to the system this

method gives an excellent overview of the nature of solutions [37]. It is one of the strongest approximate methods, which has been successfully applied to solve numerous systems like Helmholtz equation, Broer-Kaup (BK) systems, Whitham Broer-Kaup (WBK) systems [38], cubic-quintic Duffing oscillators [39], and periodic solutions of some nonlinear oscillators with strong nonlinearity [29]. The layout of this paper is as follows. In section 2 we presented the mathematical model. Section 3 contains the results and discussions, which is followed by a brief conclusion.

2. Mathematical model

At steady state, the pulse dynamics in a laser cavity, usually VCSEL, coupled with FSF is represented by the following CGLE [22]:

$$\left(\frac{\partial}{\partial t} + 1 \right) E(x,t) - i \frac{\partial^2 E(x,t)}{\partial x^2}$$
$$- \mu(1 - i\alpha)(1 - |E|^2)E(x,t) \qquad (1)$$
$$- \sigma(a - ib)E(x,t) = 0$$

where, $E(x,t)$ is the slowly varying wave envelope of the electric field of the laser pulse, t is cavity round trip time and x is the coordinate transverse to the cavity axis. Here, $a = \Gamma_0 /(\Gamma_0^2 + \Omega_0^2)$, $b = \Omega_0 /(\Gamma_0^2 + \Omega_0^2)$, while Ω_0 represents resonant frequency and Γ_0 is the line-width enhancement parameter of the feedback field. σ represents the coupling constant or feedback strength. μ represents scaled gain that is responsible for the stabilization of the off-state in VCSEL. The line-width enhancement parameter α usually attains large positive values for VCSEL. In equation (1), the first term represents evolution of the wave envelope $E(x,t)$ and linear loss inside the cavity. The second term is the diffraction term. The third term contains Kerr nonlinearity and nonlinear loss/gain (depending upon the sign of the coefficients) incurred in the transverse direction of cavity. The last term in the equation represents the contribution of frequency selective feedback. Equation (1) can be rewritten as a perturbed nonlinear Schrödinger equation (NLSE) as follows:

$$i \frac{\partial E}{\partial t} + \frac{\partial^2 E}{\partial x^2} - (\sigma b + \alpha\mu)E$$
$$+ \alpha\mu |E|^2 E = iR(E, E^*) \qquad (2)$$

where $R(E, E^*) = (\sigma a - 1 + \mu)E - \mu |E|^2 E$ is the perturbation term, nullifying which one can retrieve an unperturbed NLSE. Both the forms of equations (1) and (2) are well explored in different fields of study, particularly, in cavity dynamics. In the present investigation, we introduce the following perturbation term:

$$R(E, E^*) = \frac{\partial}{\partial x} \left[(\sigma a - 1 + \mu)E - \mu |E|^2 E \right] \qquad (3)$$

The above form represents the slope of the perturbation, which has been used in anticipation to include the effect of modulation of perturbation in a spatially distributed system. Alternatively, the two terms represent inter-modal dispersion as well as self-steepening effect. This slope could add a pseudo 3D effect in the resultant soliton profile, which may be even better than an actual 3D profile as far as visualization is concerned.

In order to find the 1-soliton traveling wave solution we consider the following ansatz [27, 29]:

$$E(x,t) = \psi(s) \exp\left(i(-kx + \omega t + \theta) \right) \qquad (4)$$

where $\psi(s)$ represents the pulse shape, $s = x - vt$, v is the velocity of the soliton, k is the soliton wave number, ω is the soliton frequency and θ is the phase constant. Hereafter we will refer $\psi(s)$ as profile function. Substituting equation (4) in equation (2) that incorporates the new perturbation term given by equation (3) and separating the real and imaginary parts, we obtain the following set of equations:

$$\psi'' + (-\omega - \sigma b + k^2 - \alpha\mu)\psi + \alpha\mu\psi^3$$
$$= k(\sigma a - 1 + \mu)\psi + \mu k \psi^3 \qquad (5)$$

and

$$(-2k - v)\psi' = (\sigma a - 1 + \mu)\psi' - 3\mu\psi^2\psi' \qquad (6)$$

where $\psi' = d\psi / ds$ and $\psi'' = d^2\psi / ds^2$. Solving equation (6) for ψ we get,

$$\psi = \pm\sqrt{\frac{v + 2k + \sigma a - 1 + \mu}{3\mu}} \qquad (7)$$

Equation (7) indicates that the soliton solution exists iff $3\mu (v + 2k + \sigma a - 1 + \mu) > 0$. Therefore, for any acceptable profile function ψ, the wave velocity needs to satisfy the following relation:

$$v > (1 - 2k - \sigma a - \mu) \qquad (8)$$

Taking into account the limiting condition of velocity, as stated in equation (8), the velocity of the traveling wave can be kept constant. The velocity need to be a positive quantity. For a suitable choice of parameters (α=2.7, μ=1.397, σ = 0.7, $\Gamma_0 = 0.5$ and $\Omega_0 = 0.1$) and obeying the inequality relation as stated in equation (8), we consider $v = 2.7568$, which we used throughout the investigation. Multiplying equation (5) by ψ' and then integrating it over the entire space, we obtain:

$$\frac{\psi'^2}{2} + (-\sigma b - \omega + k^2 - \alpha\mu - \sigma a + 1 - \mu)\frac{\psi^2}{2}$$
$$+ (\alpha\mu - \mu k)\frac{\psi^4}{4} = K \qquad (9)$$

where, K is the constant of integration. For this system, a new quantity J can be defined as follows [30]:

$$J = \int_{-\infty}^{\infty} K ds \qquad (10)$$

On substituting equation (9) in equation (10), we get

$$J = \int_{-\infty}^{\infty} \left(\begin{array}{c} \dfrac{\psi'^2}{2} + (\alpha\mu - \mu k)\dfrac{\psi^4}{4} \\[2mm] + (-\sigma b - \omega + k^2 - \alpha\mu - \sigma a + 1 - \mu)\dfrac{\psi^2}{2} \end{array} \right) ds \qquad (11)$$

A proper choice of the profile function $\psi(s)$ is now required to proceed further.

3. Results and discussion

To solve equation (1) we consider two different profile functions. One is hyperbolic secant ($sech$) function; a widely studied standard function for bright soliton and the other is a cosh-Gaussian function; an exotic function. The former is adopted to reveal the nature of the basic TW solution, while the latter is considered in the anticipation of achieving a versatile TW profile.

Case-I: sech profile function

The fundamental modes emitted by lasers are generally modelled as either ' $sech$ ' or Gaussian type. $sech$ function is the exact solution of an unperturbed cubic NLSE. Gaussian function is also equally popular for the ease of mathematical modelling and calculations without altering the physics behind. In the present case we choose the standard $sech$ type (bright) one-soliton solution of the following form:

$$\psi(s) = P\, sech(Rs) \qquad (12)$$

The parameters P and R represent the amplitude and inverse of the width of soliton respectively. Our primary target is to determine the values of P and R. Substituting equation (12) in equation (11), we obtain

$$J = \frac{P^2 R}{3} + \mu(\alpha - k)\frac{P^4}{3R}$$
$$+ (-\sigma b - \omega + k^2 - \alpha\mu - \sigma a + 1 - \mu)\frac{P^2}{R} \qquad (13)$$

The values of P and R can be obtained, using the principle of variation, i.e., $\partial J / \partial P = 0$ and $\partial J / \partial R = 0$. These conditions in conjugation with equation (13) lead to the following relations:

$$R^2 + 3(-\sigma b - \omega + k^2 - \alpha\mu - \sigma a + 1 - \mu)$$
$$+ 2(\alpha - k)\mu P^2 = 0 \qquad (14)$$

and

$$-R^2 + 3(-\sigma b - \omega + k^2 - \alpha\mu - \sigma a + 1 - \mu)$$
$$+ (\alpha - k)\mu P^2 = 0. \qquad (15)$$

On solving equations (14) and (15), we obtain

$$P = \sqrt{\frac{2(-\sigma b - \omega + k^2 - \alpha\mu - \sigma a + 1 - \mu)}{\mu(k - \alpha)}} \qquad (16)$$

and

$$R = \sqrt{(-\sigma b - \omega + k^2 - \alpha\mu - \sigma a + 1 - \mu)} \qquad (17)$$

Therefore, the final 1-soliton TW solution for the VCSEL-FSF system reads as:

$$E(x,t) = \sqrt{\frac{2(-\sigma b - \omega + k^2 - \alpha\mu - \sigma a + 1 - \mu)}{\mu(k - \alpha)}}$$
$$\times sech\left\{ \sqrt{(-\sigma b - \omega + k^2 - \alpha\mu - \sigma a + 1 - \mu)}\, s \right\} \qquad (18)$$
$$\times \exp(i(-kx + \omega t + \theta))$$

Fig. 1 depicts the intensity profile of the sech 1-soliton solution. This solution is found to be valid for a large choice of system parameters.

Case-II: Exotic cosh-Gaussian profile function

We now explore the possibility to achieve soliton solution with a profile different from the standard $sech$ form. We consider cosh-Gaussian profile function of the following form as an ansatz for the system:

$$\psi = A\cosh(Bs)\exp\left(-\frac{s^2}{T^2}\right) \qquad (19)$$

Here, A represents the pulse amplitude, B is the cosh parameter and T represents the pulse width. This type of pulse can be generated by superposing two decentred Gaussian pulses [40]. This profile function is of fundamental interest because by choosing suitable cosh parameter a variety of field distribution can be achieved. At a very small value of cosh-parameter the pulse is almost Gaussian, which will transform to a deformed Gaussian, then flattop and finally to one with a central dip with increasing value of cosh-parameter. Cosh-parameter also decides the steepness of the profile, which in turn influences other optical localized structures nearby. Thus the cosh-parameter renders a controlling tool and hence has potential applications in all-

optical tunable devices [41]. Besides, a large 3D cosh-Gaussian function, which is of annular intensity profile may trap a small optical structure and, in principle, quantum particles.
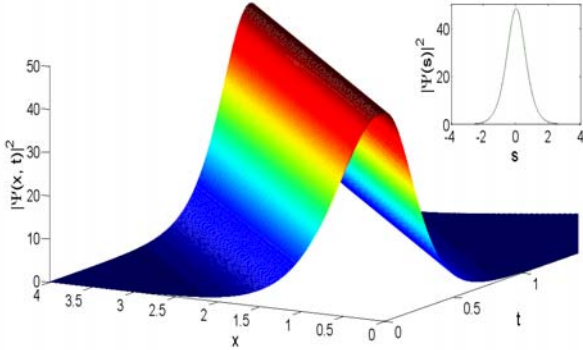

Fig. 1. 3D profile of sech traveling wave soliton solution. Inset shows 2D profile, i.e., cross-section of the 3D profile. Here, α=2.7, μ=1.397, σ=0.7, Γ_0 =0.5

and Ω_0 =0.1.

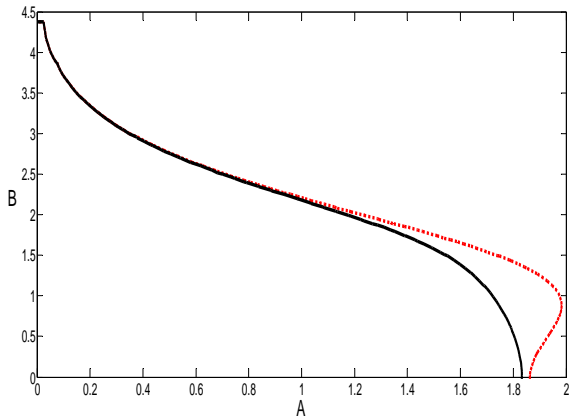*Fig. 2. Plots of equations (21)-(22) with T=1.02. The long intersecting/ overlapping region corresponds to the stable soliton solution.*

Now, substituting the cosh-Gaussian shape function, i.e., equation (19) in equation (11), we obtain the following relation for J:

$$J = -\frac{\sqrt{2\pi}A^2}{8T}\left(B^2T^2 - e^{\frac{B^2T^2}{2}} - 1\right)$$

$$+ \frac{\sqrt{2\pi}}{8}(-\sigma b - \omega + k^2 - \alpha\mu - \sigma a + 1 - \mu)A^2T\left(e^{\frac{B^2T^2}{2}} + 1\right)$$

$$+ \frac{\sqrt{\pi}\mu(\alpha - k)A^4T}{16}\left(e^{B^2T^2} + 4e^{\frac{B^2T^2}{4}} + 3\right).$$

(20)

Like the case of sech solution the values of A, B and T can be determined by varying J with respect to each system parameter, i.e., $\partial J / \partial A = 0$, $\partial J / \partial B = 0$ and $\partial J / \partial T = 0$. These yield the following equations respectively,
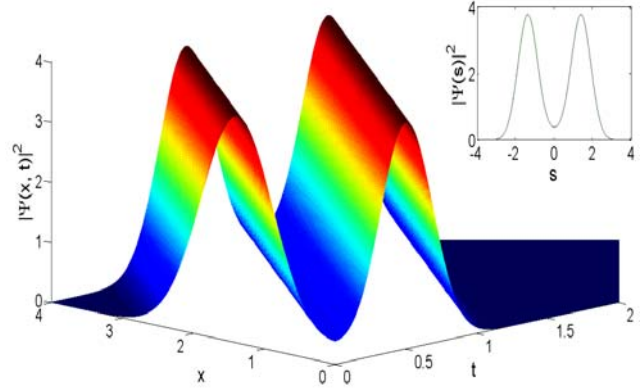

Fig. 3. Traveling wave soliton solution of cosh-Gaussian profile. A=0.6236, B= 2.6505 and T=1.02. 2D profile is in the inset. Here, α=2.7, μ=1.397, σ=0.7, Γ_0 =0.5 and Ω_0 =0.1. Cosh-Gaussian nature of profile is evident from the dip between the two humps.
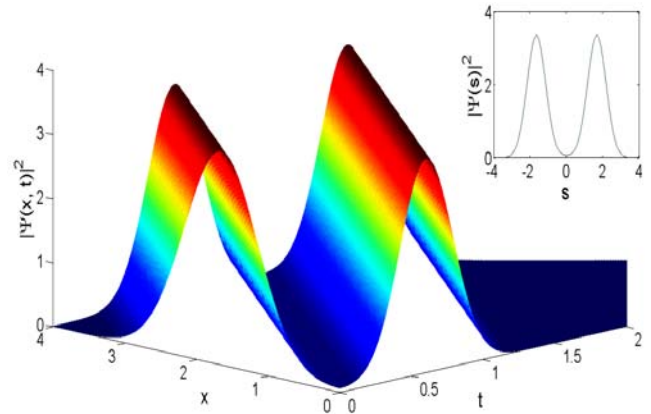

Fig. 4. Cosh-Gaussian traveling wave soliton solution for A=0.2599, B=3.1874, T=1.02. 2D profile is in the inset. As A decreases and B increases, the dip tends to touch the bottom line. The values of α, μ, σ, Γ_0 and Ω_0 are same as in fig. 3.

$$\sqrt{2}(-\sigma b - \omega + k^2 - \alpha\mu - \sigma a + 1 - \mu)T^2\left(e^{\frac{B^2T^2}{2}} + 1\right)$$

$$- \sqrt{2}\left(B^2T^2 - e^{\frac{B^2T^2}{2}} - 1\right)$$

$$+ \mu(\alpha - k)A^2T^2\left(e^{B^2T^2} + 4e^{\frac{B^2T^2}{4}} + 3\right) = 0$$

(21)

$$\sqrt{2}(-\sigma b - \omega + k^2 - \alpha\mu - \sigma a + 1 - \mu)T^2 e^{\frac{B^2T^2}{2}}$$

$$-\sqrt{2}\left(2 - e^{\frac{B^2T^2}{2}}\right) \tag{22}$$

$$+ \mu(\alpha - k)A^2 T^2 \left(e^{B^2T^2} + e^{\frac{B^2T^2}{4}}\right) = 0$$

and

$$\frac{\sqrt{2}}{T^2}\left(B^2 T^2 - e^{\frac{B^2T^2}{2}} - 1\right) - \sqrt{2}B^2\left(2 - e^{\frac{B^2T^2}{2}}\right)$$

$$+ \sqrt{2}m\left(e^{\frac{B^2T^2}{2}} + 1\right) + \sqrt{2}mB^2T^2 e^{\frac{B^2T^2}{2}}$$

$$+ \frac{\mu}{2}(\alpha - k)A^2\left(e^{B^2T^2} + 4e^{\frac{B^2T^2}{4}} + 3\right) \tag{23}$$

$$+ \mu(\alpha - k)A^2 B^2 T^2\left(e^{B^2T^2} + 4e^{\frac{B^2T^2}{4}}\right) = 0$$

The solutions of equations (21) - (23) give the values of A, B and T. Solving the equations (21)-(23) analytically is a cumbersome process. Therefore, solving numerically, Fig. 2 depicts the plot of equations (21) & (22), for a constant value of T. The intersections are the solutions of equation (21) and (22). In fig. 2, instead of few discrete solution points we get a long overlapping region that signifies a large family of parametric solution. The curves intersect at region where value of A is less than 1. Any point on the intersecting region, with the fixed T-value corresponds to a possible solution of the system.

Considering the different solution points from fig. 2, different solution profiles are plotted. For the point considering values $A = 0.6236$, $B = 2.6505$ and $T = 1.02$, a 3D cosh-Gaussian function profile is plotted, which is shown in fig. 3. Inset shows the corresponding 2D profile with same parametric values. It is evident from the figure that the pulse propagates as a stable soliton with a central dip. Figs. 4 and 5 show the cosh-Gaussian profile functions with ($A = 0.2599$, $B = 3.1874$) and ($A = 0.0255$, $B = 4.3832$) respectively at constant T = 1.02. As the value of A decreases and B increases, the dip between two humps changes its shape and depth, which is clearly evident from the inset of figures 3, 4 and 5, respectively.
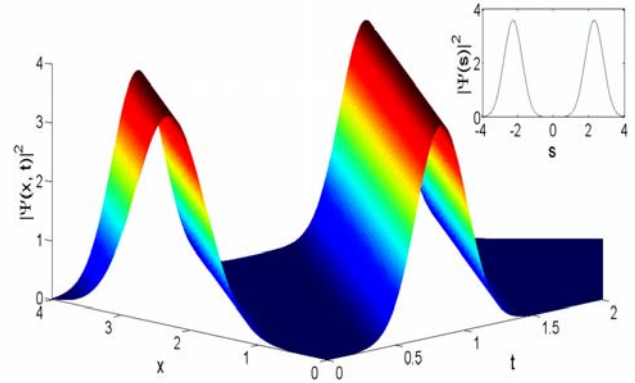

Fig. 5. Cosh-Gaussian traveling wave soliton solution for A=0.0255, B=4.3832, T=1.02. Inset is the corresponding 2D profile. A greater value of B broadens the dip significantly, which is clearly evident in 2D profile. The values of α, μ, σ, Γ_0 and Ω_0 are same as in fig. 3.

4. Stability analysis

For understanding the dynamics of any system, stability analysis is an essential routine. Thus we now analyse the stability of the solutions obtained in the previous section. At steady state the system described by equation (2) in conjugation with equation (3) obeys the following conditions: $\partial^2 E/\partial x^2 = 0$, $\partial E/\partial x = 0$. We consider, $E = E_0 = \sqrt{I_0}e^{i\omega t}$. This results into:

$$\omega = -(\sigma b + \mu\alpha) + \mu\alpha I_0 \tag{24}$$

A small perturbation is now added to the system as follows: $E = E_0 + \delta E e^{iqx}$. Substitution of the perturbed wave function E in equations (2) and (3) and subsequent linearization around the stationary values result in a pair of coupled equations:

$$\frac{\partial Q}{\partial t} = -i(q^2 + (\sigma b + \mu\alpha) + (\sigma a - 1 + \mu)q$$
$$+ 2\mu\alpha I_0^2 - 2\mu q I_0)Q + i(\alpha\mu + q)E_0 Q^* \tag{25}$$

$$\frac{\partial Q^*}{\partial t} = i(q^2 + (\sigma b + \mu\alpha) + (\sigma a - 1 + \mu)q$$
$$+ 2\mu\alpha I_0^2 - 2\mu q I_0)Q^* - i(\alpha\mu + q)E_0 Q \tag{26}$$

where $Q = \delta E e^{iqx}$ and $Q^* = \delta E^* e^{-iqx}$. Equations (25) and (26) can be put in the matrix form as

$$\frac{\partial}{\partial t}\begin{bmatrix} Q \\ Q^* \end{bmatrix} = \begin{bmatrix} A & B \\ B^* & A^* \end{bmatrix}\begin{bmatrix} Q \\ Q^* \end{bmatrix} \tag{27}$$

where

$$A = i(q^2 + (\sigma b + \mu\alpha) + (\sigma a - 1 + \mu)q \\ + 2\mu\alpha I_0^2 - 2\mu q I_0) \tag{28}$$
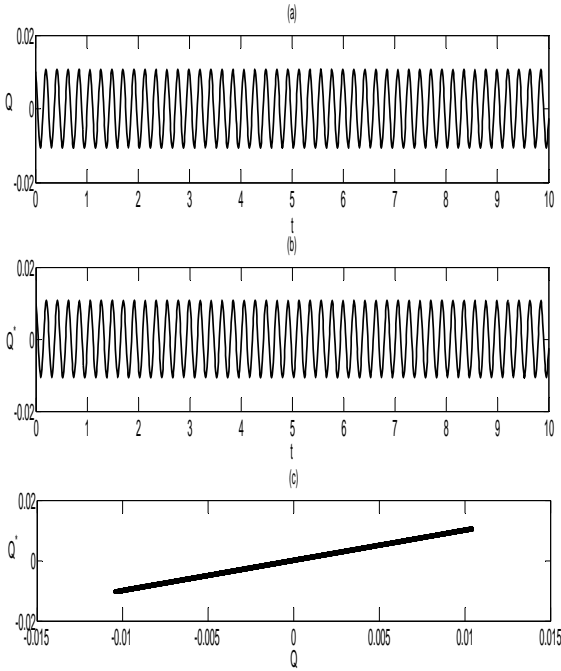
and

$$B = -i(\alpha\mu + q) \tag{29}$$

Fig. 6. Bound oscillation for the system described by equations (25) and (26) for parameter set same as in figure 1. (a) and (b) shows the evolution of Q and Q* with respect to t, respectively and (c) shows the phase plot of Q and Q* during the evolution.

A* and B* are complex conjugates of A and B respectively. Eigen values for equation (27) are given by:

$$\lambda^2 - 2\operatorname{Re}(A)\lambda + |A|^2 - |B|^2 = 0 \tag{30}$$

or

$$\lambda = \operatorname{Re} A \pm \sqrt{(\operatorname{Re}(A))^2 + |B|^2 - |A|^2} \tag{31}$$

Since $\operatorname{Re}(A)$ is zero and $|A| > |B|$ both the Eigen values are purely imaginary. Further, as the real parts of the Eigen values are zero, the fixed points are neutrally stable. Thus, in the neighbourhood of the fixed point, soliton parameters will oscillate around the steady state value. Time evolution of Q and Q^* are obtained by solving equations (25) and (26) numerically using Range-Kutta 45 method and depicted in figures (6a) and (6b) respectively. Both Q and Q^* shows bound periodic oscillation for the range of $\mu = (0.1, 5.5)$. Phase plot shown in figure (6c) also supports the bound motion of the system in the phase plane. As the system

parameter $\mu \to 0$, the system oscillates with a very large amplitude thus pushing the system towards instability. Figure 7 shows the unbound dynamics of the system with $\mu = 0.01$. Although, the phase portrait is bound, but with a large amplitude.
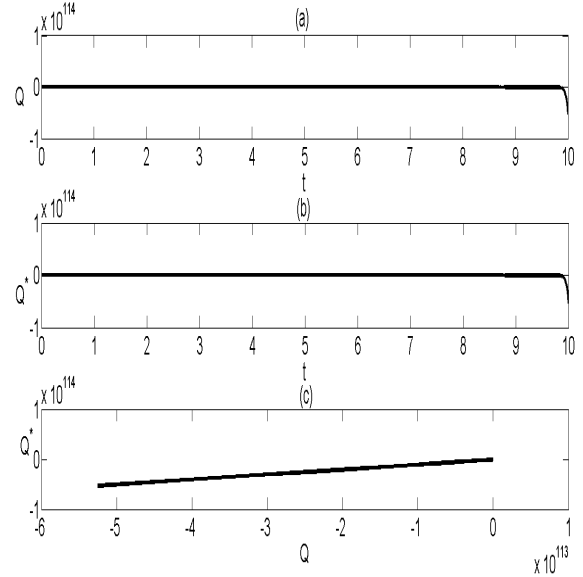

Fig. 7. Unbound dynamics of the system described by equations (25) and (26) for the same parameter set as stated in figure 1, but changing the value of $\mu = 0.01$. (a) and (b) shows the unbound evolution of Q and Q* with respect to t, respectively and (c) shows the phase plot of Q and Q* during the evolution. Although, phase plot seems to be bound, it actually exhibits a large amplitude of oscillation.

5. Conclusion

In this paper we derived TW soliton solutions in a VCSEL coupled with a FSF. He's semi-inverse variational method has been successfully used to obtain a sech type and an exotic cosh-Gaussian type soliton solution by solving the governing CGLE. We identified a parametric region that yield a large family of stable soliton solutions. The versatile profile of cosh-Gaussian type soliton solution is of fundamental interest as well as can be utilized for tuning and controlling the system behaviour. Such soliton solutions have potential applications in fabrication of all-optical devices, data processing and controlling units, optical memories, delay lines and optically addressable displays. Moreover, a 3D cosh-Gaussian distribution with annular intensity profile may trap a small optical structure even quantum particles.

References

[1] T. Ackemann, W. J. Firth, G. L. Oppo, Advances in Atomic, Molecular and Optical Physics. San Diego, USA: Academic Press, **57**, 323 (2009)

[2] W. J. Firth, G. K. Harkness, Asian Journal of Physics, **7**, 665 (1998)

[3] S. Barland, J. R. Tredicce, M. Brambilla, L. A. Lugiato, S. Balle, M. Giudici, T. Maggipinto, L. Spinelli, G. Tissoni, T. Knödl, M. Miller, R. Jäger, Nature, **419**, 699 (2002)

[4] W. J. Firth, C. O. Weiss, Opt and Photon News, 13, 54 (2002)

[5] P. Manneville, Dissipative Structures and Weak Turbulence. Academic press: Boston; 1990.

[6] R. Richter, I. V. Barashenkov, Phys Rev Lett. **94**, 184503 (2005)

[7] D. Mihalache, D. Mazilu, F. Lederer, Y. V. Kartashov, L. C. Crasovan, L. Torner, B. A. Malomed, Phys Rev Lett. **97**, 073904 (2006)

[8] I. Müller, E. Ammelt, H. G. Purwins, Phys Rev Lett. **82**, 3428 (1999)

[9] J. D. Murry, Mathematical Biology: Spatial models and biomedical applications, Springer-Verlag: Berlin; 2003.

[10] J. Ross, S. C. Müller, C. Vidal, Science, **240**, 460 (1998)

[11] A. P. Stamp, M. Jacka, J Fluid Mech. **305**, 347 (1995)

[12] N. Akhmediev, A. Ankiewicz, Dissipative Solitons. Vol. 661, Lecture Notes in Physics. Springer-Verlag: Berlin; 2005.

[13] N. Akhmediev, A. Ankiewicz, Dissipative Solitons: From Optics to Biology and Medicine. Vol. 751, Lecture Notes in Physics. Springer-Verlag: Berlin; 2008.

[14] Z. Chen, M. Segev, Rep Prog Phys. **75**, 086401 (2012)

[15] W. J. Firth, Theory of Cavity Solitons. In: AD Boardman, AP Sukhorukov editors. Soliton Driven Photonics. Netherlands: Kluwer Academic Publishers; p. 459, 2009.

[16] N. N. Rosanov, G. V. Khodova, Opt and Spectr. **65**, 449 (1988)

[17] S.V. Fedorov, A. G. Vladimirov, G. V. Khodova, N. N. Rozanov, Quant Electron. **27**, 949 (1997)

[18] E. A. Ultanir, G. I. Stegeman, D. Michaelis, C. H. Lange, F. Lederer, Phys Rev Lett. **90**, 253903 (2003)

[19] Z. Bakonyi, D. Michaelis, U. Peschel, G. Onishchukov, F. Lederer, J Opt Soc Am B. **19**(3), 487 (2002)

[20] N. Radwell, T. Ackemann, IEEE J Quant Electron. **45**(11), 1388 (2009)

[21] M. Bache, F. Prati, G. Tissoni, R. Kheradmand, L. A. Lugiato, I. Protsenko, M. Brambilla, Appl Phys B, **81**(7), 913 (2005)

[22] W. J. Firth, P. V. Paulau, Eur Phys J D, **59**, 13 (2010)

[23] A. J. Scroggie, W. J. Firth, G. L. Oppo, Phys Rev A, **80**, 013829 (2009)

[24] V. Skarka, N. B. Aleksic, H. Leblond, B. A. Malomed, D. Mihalache, Phys Rev Lett. **105**, 213901 (2010)

[25] E. N. Tsoy, A. Ankiewicz, N. Akhmediev, Phys Rev E, **73**, 036621 (2003)

[26] F. Abdullaev, V. V. Konotop, M. Salerno, A. V. Yulin, Phys Rev E, **82**, 056606 (2010)

[27] A. Zavyalov, R. Iliew, O. Egorov, F. Lederer, Phys Rev A, **79**, 053841 (2009)

[28] P. V. Paulau, A. J. Scroggie, A. Naumenko, T. Ackemann, N. A. Loiko, W. J. Firth, Phys Rev E, **75**, 056208 (2007)

[29] A. Amani, D. D. Ganji, A. A. Jebelli, M. Shahabi, N. S. Nosar, Int. J. Appl. Math. Comput. **2**(3), 33 (2010)

[30] A. Biswas, Progress in Electromagnetics Research, **96**, 1 (2009)

[31] A. Biswas, S. Johnson, M. Fessak, B. Siercke, E. Zerrad, S. Konar, J Mod Opt. **59**(3), 213 (2012)

[32] A. Biswas, Quant Phys Lett. **1**(2), 79 (2012)

[33] A. Biswas, D. Milovic, D. Michelle, M. Savescu, M. F. Mahmood, K. R. Khan, R. Kohl, J. Nonlinear Opt. Phys. Mat. **12**(4), 1250054 (2012)

[34] R. Kohl, D. Milovic, E. Zerrad, A. Biswas, J. Infrared Milli Terahz Waves. **30**, 526 (2009)

[35] A. H. Bhrawy, A. A. Alshaery, E. M. Hilal, K. R. Khan, M. F. Mahmood, A. Biswas, Optik, **125**(17), 4945 (2014)

[36] A. Biswas, D. Milovic, R. Kohl, Inverse Problems in Science and Engineering, **20**(2), 227 (2012)

[37] Z. L. Tao, Zeitschrift für Naturforschung, **63**(a), 634 (2008)

[38] M. El-Sabbagh, S. El-Ganaini, International Mathematical Forum, **7**, 2131 (2012)

[39] S. S. Ganji, D. D. Ganji, H. Babazadeh, S. Karimpour, Progress in Electromagnetics Research M, **4**, 23 (2008)

[40] S. Konar, S. Jana, Opt Commun. **236**, 7 (2004)

[41] S. Jana, S. Konar, Opt Commun. **267**, 24 (2006)

*Corresponding author: soumendujana@yahoo.com